Journal of Sound and Vibration (2001) **248**(5), 963–974
doi:10.1006/jsvi.2001.3722, available online at http://www.idealibrary.com on IDEAL®

VISUALIZING SOUND RADIATION FROM A VEHICLE FRONT END USING THE HELS METHOD

S. F. Wu and N. E. Rayess

Department of Mechanical Engineering, Wayne State University, Detroit, MI 48202 *U.S.A.*

AND

N.-M. Shiau

Advanced Engineering Center, Ford Motor Company, Dearborn, MI 48121 *U.S.A.*

(*Received* 1 *September* 2000, *and in final form* 30 *April* 2001)

1. INTRODUCTION

The automotive industry has constantly been pursuing ways to reduce the vehicle noise and vibrations in response to the ever-increasing customer demand on comfort and government regulation on noise emission. Despite all attempts to incorporate noise, vibration, and harshness (NVH) reduction into the early design stages, the complexity of a vehicle ensures that many problems go unnoticed until after a prototype is built. Under these circumstances, the attention often shifts to minimizing the propagation of sound and vibration. Therefore, it is highly desirable to have an effective means to identify where and how noise is transmitted into the passenger compartment as well as to the outside.

Over the past two decades, many methodologies have been developed to tackle this type of problems. One such method is called spatial transform of sound field (STSF) [1], which uses planar nearfield acoustic holography (NAH) to reconstruct the radiated acoustic pressure field [2–4]. The use of planar NAH, however, limits the spatial transformation of sound fields between planar surfaces. Moreover, the measurements must be equidistantly spaced on a plane and the measurement aperture must be large enough to form a 45° solid angle with respect to the source under consideration. These restrictions severely limit the application of STSF because in engineering applications, the actual surface of a structure is often arbitrary. Also, the presence of accessory components of a structure may conflict or interfere with the placement of a microphone array. Consequently, one is often forced to take measurements at certain distances away from the structure in order to avoid these obstacles. The accuracy of the resultant reconstruction is therefore compromised because the nearfield effects are lost in the input data.

Another method is the Helmholtz integral theory based NAH [5–8]. Thus far, however, this methodology has not been embraced by the industry and its usage has been mainly limited to the research laboratories. The main reasons for that are its heavy reliance on spatial sampling and the requirement that measurements be taken over an enclosure completely surrounding the source under consideration. To avoid aliasing in reconstruction, the sound field must be sampled at a minimum rate of twice per wavelength. The number of field measurements must be comparable to the number of discretized nodes

0022-460X/01/500963 + 12 $35.00/0 © 2001 Academic Press

on the source surface, which can easily run into hundreds for a complex structure such as an engine block. While there is no restriction on the locations of measurements, the high number of required measurements surrounding the source surface can make the reconstruction process very slow and costly.

The work presented here is based on the Helmholtz equation least-squares (HELS) method [9, 10]. While the HELS method is approximate, the resultant reconstruction has been shown to be quite accurate even for an arbitrarily shaped structure that contains sharp corners and edges [11, 12]. Furthermore, it requires a relatively small number of measurements over any surface (planar or non-planar) and reconstruction can be done on a piecewise basis. These unique features make this methodology a practical alternative to other methods.

The main objective of this paper is to demonstrate the application of the HELS method for reconstruction of acoustic radiation from a replicated vehicle front end based on simple acoustic pressure measurements. The acoustic field thus obtained enables one to visualize the paths through which acoustic pressures propagate from the engine to the exterior region.

The structure under consideration has the same shape and size as a full-size passenger vehicle front end. To simulate engine noise, an engine noise simulator (ENS) is installed inside the vehicle structure at the location of the engine. This ENS is a solid object that has the shape of an engine and gearbox with many loudspeakers on all sides, each emitting white noise. The acoustic pressures radiated from the ENS may excite the structure into vibrations and cause structure-borne sounds. Owing to the complexity of the structure, the vibration response cannot be described analytically. Also, the excitation forces acting on the structure from the inside are unknown. Hence, there is no way of determining the radiation impedance and efficiency precisely.

2. THE HELS FORMULATIONS

The HELS method assumes that the radiated acoustic pressure is expressible in terms of an expansion of basis functions (detailed derivations are given in references [9] and [11] and only a brief outline is given here):

$$\hat{p}(\mathbf{x}, \omega) = \sum_{j=1}^{J} C_j(\omega)\, \Psi_j(\mathbf{x}, \omega), \tag{1}$$

where $\hat{p}(\mathbf{x}, \omega)$ is the complex amplitude of the acoustic pressure at an exterior point $\mathbf{x}$, and Ψ_j are the basis functions obtained by Gram–Schmidt orthonormalization of the particular solutions ψ_i to the Helmholtz equation with respect to the source surface:

$$\Psi_j(\mathbf{x}, \omega) = \psi_j(\mathbf{x}, \omega) - \sum_{i=1}^{j} \langle \psi_j(\mathbf{x}_B, \omega),\ \Psi_i(\mathbf{x}_B, \omega) \rangle\, \Psi_i(\mathbf{x}_B, \omega), \tag{2}$$

where the inner product is defined by

$$\langle \psi_i(\mathbf{x}_B, \omega),\ \Psi_j(\mathbf{x}_B, \omega) \rangle = \int_{\partial} \int_{B} \psi_i(\mathbf{x}_B, \omega)\, \Psi_j(\mathbf{x}_B, \omega)\, \mathrm{d}S. \tag{3}$$

The particular solution ψ_i can be expressed in any spheroidal co-ordinates [13]. In the spherical co-ordinates, ψ_i can be written as

$$\psi_i(\mathbf{x}, \omega) = \psi_{n,m}(r, \theta, \phi, \omega) = h_n(kr) P_{n,m}(\cos\theta) \begin{cases} \cos(m\phi) \\ \sin(m\phi) \end{cases}, \tag{4}$$

where $h_n(kr)$ and $P_{n,m}(\cos\theta)$ denote the spherical Hankel functions and associated Legendre functions, respectively, and $k = \omega/c$ is the acoustic wave number. The existence of analytical expressions for the Hankel and associated Legendre functions in the spherical co-ordinates makes this co-ordinate system a logical choice.

The unknown coefficients C_j associated with the basis functions Ψ_j in equation (1) are determined by matching the assumed-form solution to M measured acoustic pressures $\hat{p}_m$, $m = 1, 2, \ldots, M$, leading to the linear system of equations

$$[\Psi]_{M\times J}\{C\}_{J\times 1} = \{\hat{p}_m\}_{M\times 1}. \tag{5}$$

Note that the number of measurements M must exceed the number of basis functions J. The least-squares solution can then be used to give the best fit of the unknown coefficients to the measured data:

$$\{C\}_{J\times 1} = ([\Psi]^{\mathrm{T}}_{J\times M}[\Psi]_{M\times J})^{-1}[\Psi]^{\mathrm{T}}_{J\times M}\{\hat{p}_m\}_{M\times 1}. \tag{6}$$

Once C_j are specified, the radiated acoustic pressure in the entire exterior region including the source surface can be reconstructed using equation (1).

3. EXPERIMENTAL SET-UP

The goal of this study was to develop a cost-effective diagnostic tool to visualize sound transmission from the engine compartment to the outside. With this goal in mind, a vehicle front end was designed and fabricated as shown in Figure 1. This replica, henceforth referred to as a front-end buck, has the same shape and size as a real vehicle. The windshield, tires and rear-view mirrors were removed for ease of fabrication.

The basic shape of the front-end buck was formed by a skeleton of 6 mm steel rods. This skeleton was covered by layers of wire mesh and papier-mâché, followed by another layer of joint compound. This construction yielded a surface with similar hardness and rigidity as a sheet metal. Care was taken to provide ample space inside the buck and to leave the undercarriage area unobstructed. The buck was then mounted inside an anechoic chamber at the height of a vehicle.

To simulate the engine noise, an engine noise simulator ENS (see Figure 2) was installed inside the buck at the location of the engine. The ENS was a solid structure 73 cm long, 62 cm tall, and 24 cm wide. All six sides of this ENS contained arrays of recessed speakers of different sizes and its electronics were such that each speaker emitted white noise. The ENS was controlled by a switchboard that allowed for selections of combinations of loudspeakers on all sides.

Experimental validations were conducted on the top, front, and right-hand side surfaces of the buck individually. The acoustic pressures were measured on two parallel planar surfaces, one located 12 cm away (called measurement surface) and the other 1 cm away (called reconstruction surface) from the surface of the buck (see Figure 3). The acoustic pressures collected on the measurement surfaces were used as the input to the HELS formulations to calculate the acoustic pressure spectra and distributions on the

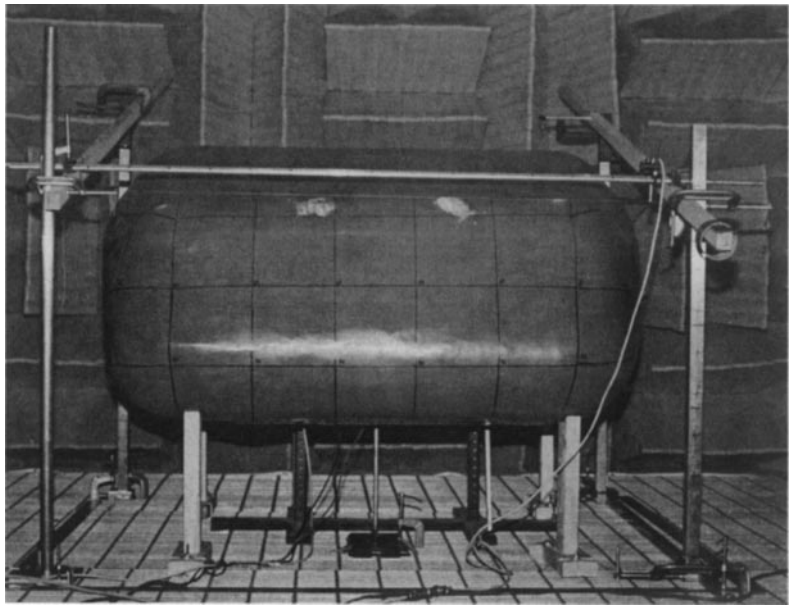

Figure 1. Experimental set-up showing the replicated vehicle front-end buck with the measurement frame inside an anechoic chamber.

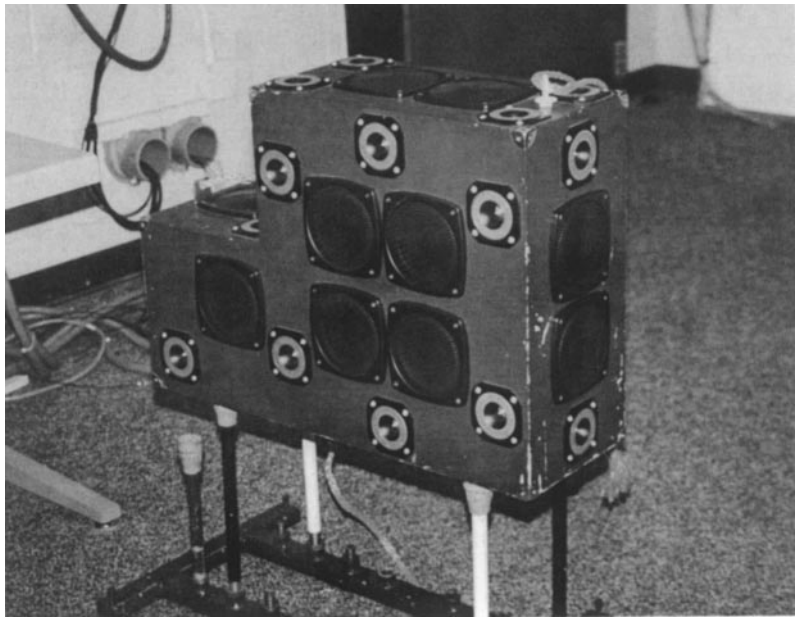

Figure 2. The engine noise simulator (ENS) system used to generate white noise inside the vehicle front-end buck.

reconstruction surfaces. The results thus obtained were compared with those measured at the same locations.

Due to the lack of a microphone array, the field acoustic pressures were collected using a single microphone. Accordingly, the microphone was moved manually from one location

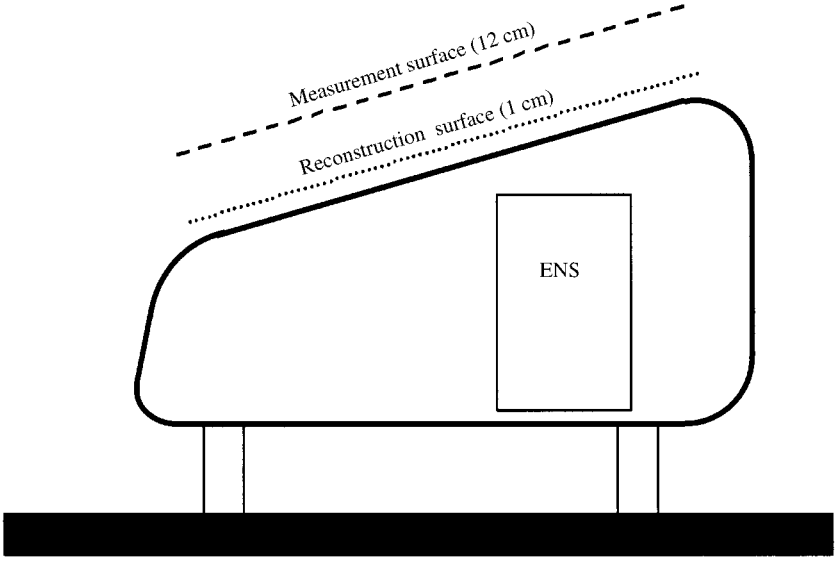

Figure 3. Schematic showing the ENS, measurement, and reconstruction surfaces in relation to the front-end buck.

to another, which prolonged the overall measurement time. To overcome a possible signal level drifting during this long period of time, transfer functions between each measurement point and a reference microphone fixed at close proximity to the ENS were measured. Once the transfer functions at all points were taken, they were multiplied by the acoustic pressure at the reference, which was equivalent to measuring acoustic pressures at all locations simultaneously.

Figure 4 shows the effect of the presence of the buck on the noise spectrum of the ENS. Without the buck, the spectrum was broadband, indicative of a typical white noise. The presence of the buck, however, completely changed the resulting noise spectrum. Measurements indicate that the buck acted as a series of band-pass filters, allowing for sound transmission at certain frequency bands that coincided with the structural resonance frequencies. Accordingly, the overall amplitude of the acoustic pressure was greatly reduced, except at certain narrowband peaks. Meanwhile, part of the acoustic energy escaped from the opening at the bottom of the structure to the exterior. Hence, the field acoustic pressure consisted of both structure-borne and airborne sounds, which were much more complicated than those emitted directly from the ENS in a free field.

4. RESULTS AND DISCUSSIONS

One unique feature of the HELS method is that it allows for a piecewise reconstruction of the acoustic pressure field based on the measurements taken over a finite aperture comparable to the size of the reconstruction. For example, the top surface of the vehicle buck was approximately 90 cm deep and 120 cm wide. In conducting reconstruction of the acoustic pressure on the top surface, the measurement aperture was set at the same size as the top surface with a 12 cm clearance. The intervals between the neighboring measurement points were 10 cm, thus resulting in 120 measurements. These measured acoustic pressures were used to determine the expansion coefficients in equation (6), then to reconstruct the

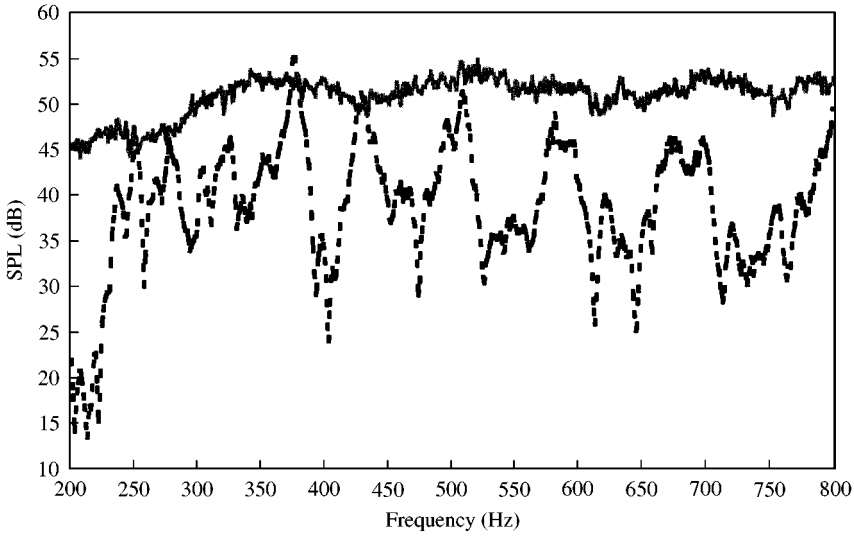

Figure 4. Effect of the vehicle front-end buck on the radiated acoustic pressure spectrum: —— without buck; – – – –, with buck.

acoustic pressure on the reconstruction surface at 1 cm atop the vehicle surface. The reconstructed acoustic pressure spectra at various locations and distributions at different frequencies were then compared with the measured data.

This procedure was repeated for the side and front panels of the buck, with the measurement apertures set at the same sizes as the side and front surfaces with a 12 cm clearance. For the given structure with a 10 cm interval between the neighboring measurement points, the total numbers of measurements were 66 and 49 respectively. This small measurement aperture is in stark contrast to planar NAH where the measurement aperture should be at least four times the size of the planar source surface [8], or to the Helmholtz integral theory based NAH where the measurement surface should enclose the entire source under consideration.

It has been shown [11] that for any given number of measurements, there is an optimal number of expansion functions J_{op} that yields the best reconstruction. The value of J_{op} depends on the signal-to-noise ratio (SNR) and the standoff distance [14]. The higher the SNR and the closer the measurement distance, the larger the value of J_{op} and the higher the accuracy of reconstruction. In this study, the optimal number of expansion functions was found to be less than 70 in all cases. This small number of expansion functions together with a small number of measurements made the numerical computations extremely fast. For example the reconstruction of a spectrum between 200 and 800 Hz can be accomplished within a couple of minutes.

Figure 5 depicts the comparison between the reconstructed and measured acoustic pressure spectra near the middle of the top surface of the buck. It is seen that satisfactory reconstruction is obtained throughout the entire frequency span of 200–800 Hz. Here, the lower bound of 200 Hz corresponds to the cut-off frequency of the anechoic chamber. The accuracy of the reconstruction at low frequencies is actually very high [14]. Hence, the truncation to the lower bound of 200 Hz was completely unnecessary. The upper frequency of 800 Hz is selected in accordance with the B&K Dual Channel Spectrum Analyzer Type 3550 so that the reconstructed acoustic pressures could be validated at every single frequency.

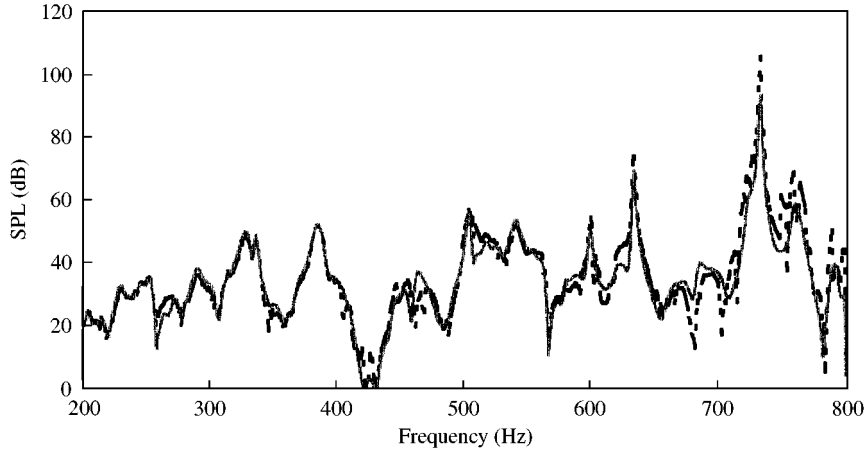

Figure 5. Comparison of the reconstructed and measured acoustic pressure spectra near the middle of the top panel of the vehicle front-end buck: ——, measured; – – – –, reconstructed.

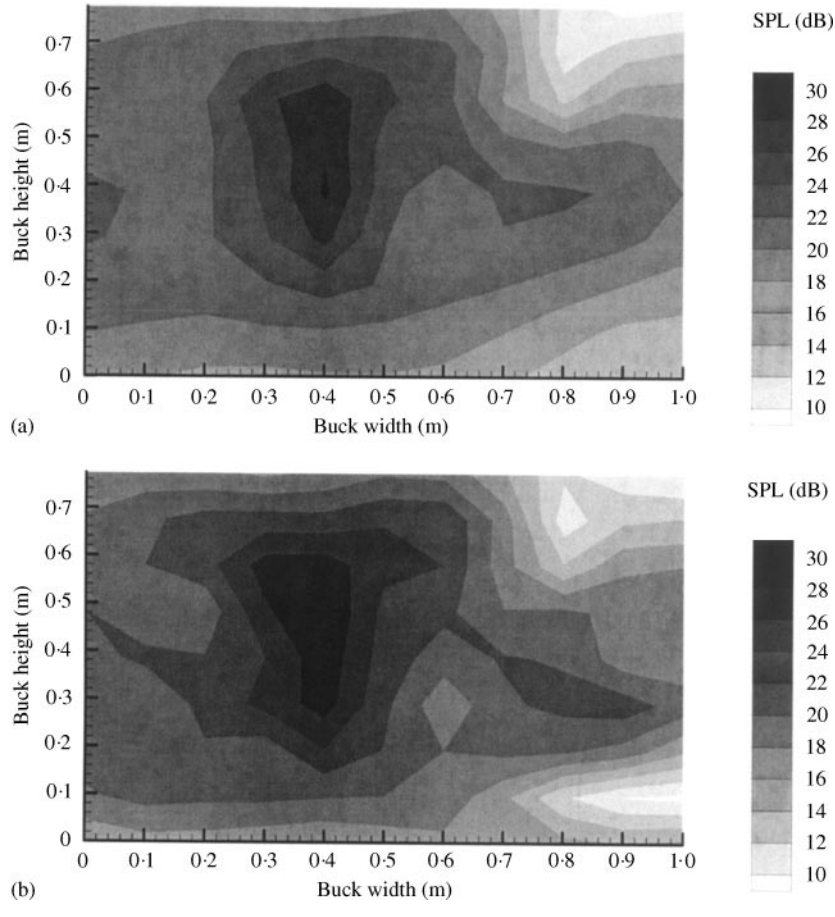

Figure 6. Acoustic pressure distribution on the top panel of the vehicle front-end buck at 204 Hz: (a) reconstructed, (b) measured.

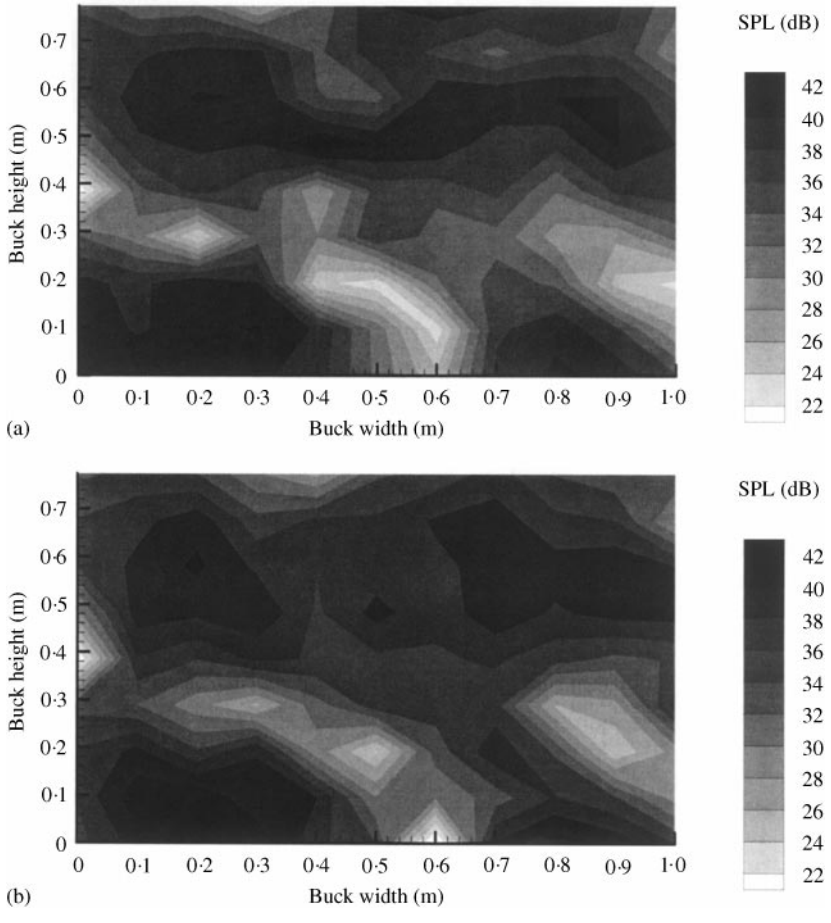

Figure 7. Acoustic pressure distribution on the top panel of the vehicle front-end buck at 457 Hz: (a) reconstructed, (b) measured.

The comparison in Figure 5 shows that an accurate reconstruction can be obtained up to at least 800 Hz or to a dimensionless frequency $ka \approx 15$, which falls in the mid-frequency regime that may present difficulties in numerical computation for many algorithms such as finite elements method (FEM) or boundary element method (BEM).

Comparisons of the reconstructed and measured acoustic pressure distributions on the top surface at 204 and 457 Hz are shown in Figures 6 and 7 respectively. The results show that at 204 Hz, the structure is relatively passive and acting primarily as a barrier. Accordingly, the resulting sound field is similar to what would exist without the presence of the buck albeit greatly attenuated. The sound field, however, is very different at 457 Hz. At this frequency, the interaction between sound and structure is strong and the buck is acting as a source with its vibration modes quite evident in the resultant acoustic pressure field.

The comparison of the measured and reconstructed spectra at a location near the middle of the front panel is shown in Figure 8. The results demonstrate that the reconstructed acoustic pressures are remarkably accurate. Figures 9 and 10 display the comparisons of the reconstructed and measured acoustic pressure distributions at 328 and 576 Hz respectively. The effect of structural vibration is even more striking in this case. At 328 Hz, the maximum acoustic pressure is found to be along the bottom edge of the front panel indicating that the

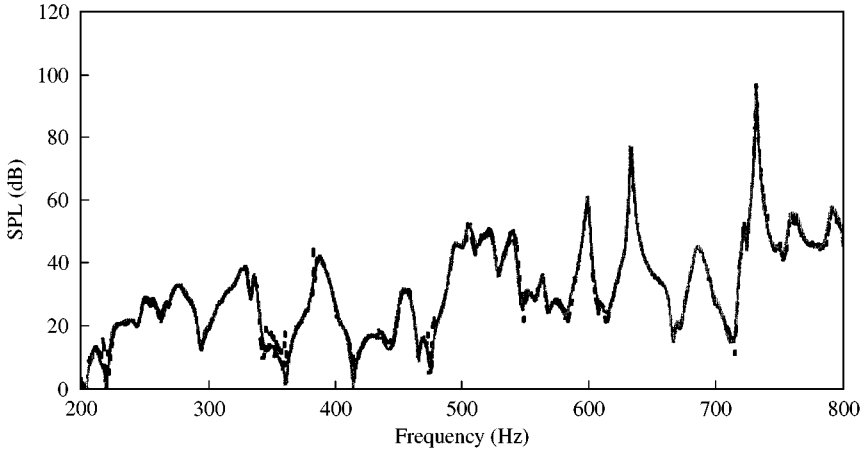

Figure 8. Comparison of the reconstructed and measured acoustic pressure spectra near the middle of the front panel of the vehicle front-end buck: ——, measured; – – – –, reconstructed.

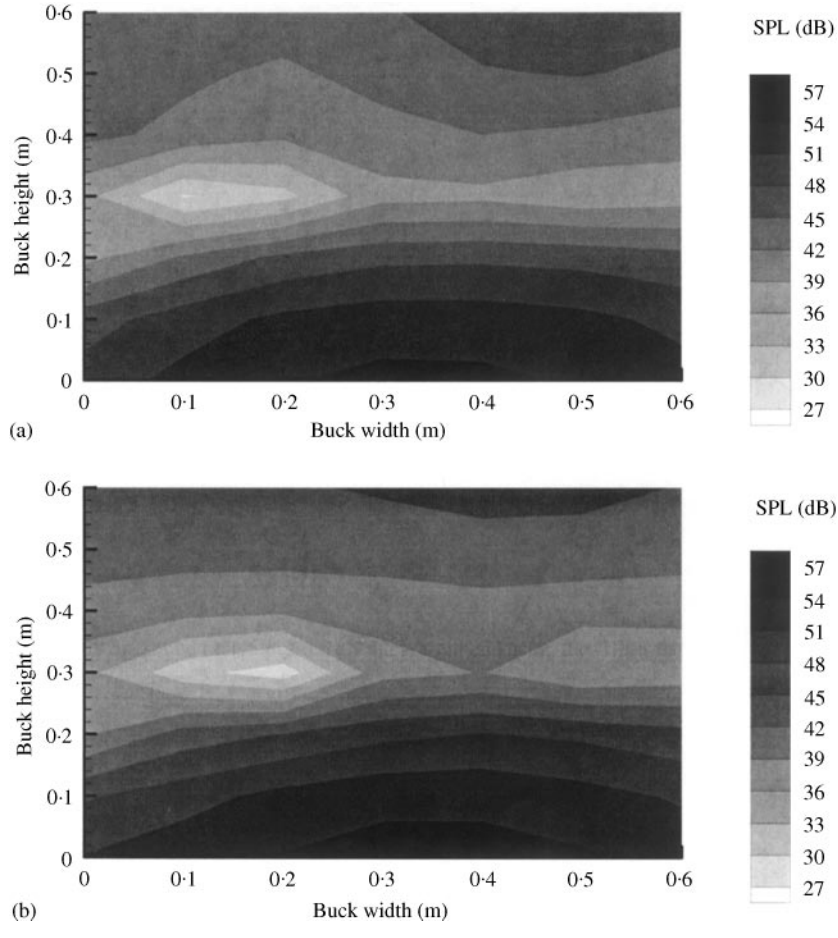

Figure 9. Acoustic pressure distribution on the front panel of the vehicle front-end buck at 328 Hz: (a) reconstructed, (b) measured.

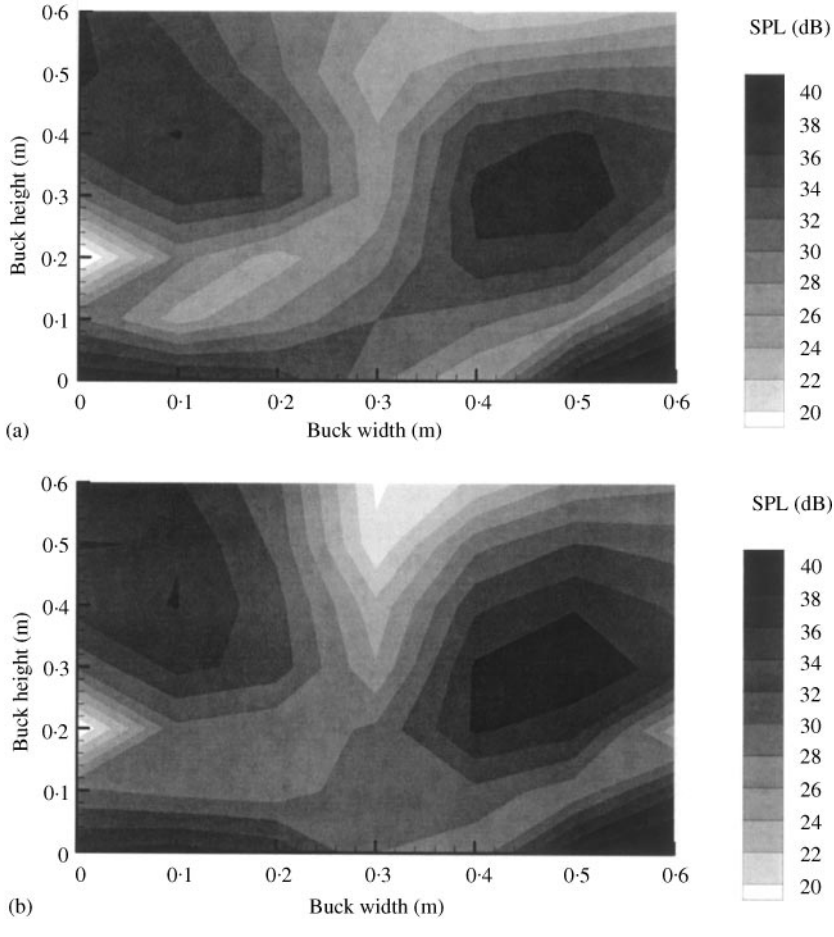

Figure 10. Acoustic pressure distribution on the front panel of the vehicle front-end buck at 576 Hz: (a) reconstructed, (b) measured.

ENS sound is transmitted primarily through the opening at the bottom of the buck. Clearly, at that frequency, the buck is simply acting as a noise barrier. On the other hand, at 576 Hz, the buck seems to be excited at one of its natural frequencies since the pressure on the surface of the buck is higher than even that at the bottom where acoustic energy is passing through unobstructed. Similar results are shown in Figure 11, which depict the reconstructed and measured acoustic pressure distributions on the side surface at 543 Hz. Once again, the structure vibration seems to be a major contributor to the external sound field at this frequency. The amplitude of the acoustic pressure in the middle is approximately the same as that at the bottom of the side panel of the buck structure.

5. CONCLUSIONS

The HELS method is shown to be capable of reconstructing the nearfield acoustic pressures radiated from a complex vibrating structure based on simple acoustic pressure measurements in the field, which consists of both structure-borne and airborne sounds. Experimental results demonstrate that the HELS method enables one to obtain piecewise

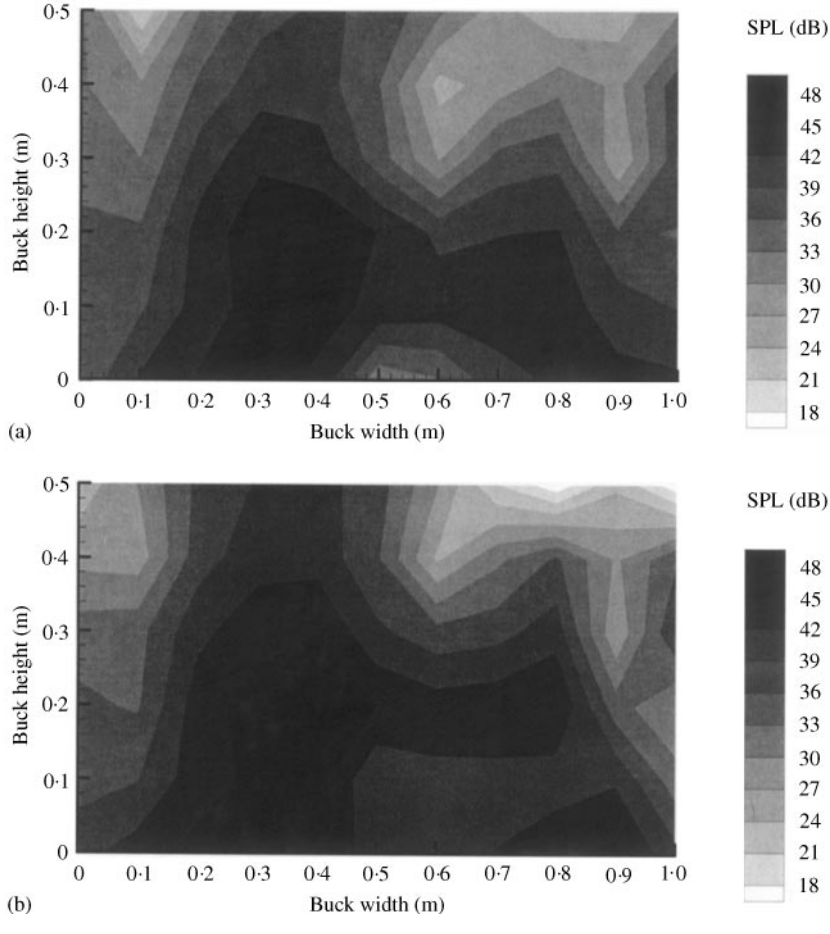

Figure 11. Acoustic pressure distribution on the side panel of the vehicle front-end buck at 543 Hz: (a) reconstructed, (b) measured.

reconstruction using a measurement aperture comparable to the size of the surface on which the acoustic pressure field is sought. This unique feature can make the HELS method very flexible and versatile in reconstructing acoustic radiation from a complex structure in engineering applications.

ACKNOWLEDGMENTS

This work was supported in part by the National Science Foundation, Grant No. CMS-9802847, and a grant from the Ford Motor Company University Research Program.

REFERENCES

1. J. HALD 1989 *Brüel & Kjær Technical Review* 1. STSF—a unique technique for scan-based near-field acoustic holography without restrictions on coherence.
2. E. G. WILLIAMS and J. D. MAYNARD 1980 *Physical Review Letters* **45**, 554–557. Holographic imaging without the wavelength resolution limit.

3. J. D. MAYNARD, E. G. WILLIAMS and Y. LEE 1985 *Journal of the Acoustical Society of America* **78**, 1395–1413. Nearfield acoustic holography I. Theory of generalized holography and the development of NAH.
4. W. A. VERONESI and J. D. MAYNARD 1987 *Journal of the Acoustical Society of America* **81**, 1307–1322. Nearfield acoustic holography (NAH) II. Holographic reconstruction and computer implementation.
5. W. A. VERONESI and J. D. MAYNARD 1989 *Journal of the Acoustical Society of America* **85**, 588–599. Digital holographic reconstruction of sources with arbitrarily shaped surfaces.
6. G. T. KIM and B. T. LEE 1990 *Journal of Sound and Vibration* **136**, 245–261. 3-D sound source reconstruction and field reprediction using the Helmholtz integral equation.
7. M. R. BAI 1992 *Journal of the Acoustical Society of America* **92**, 533–549. Application of BEM (boundary element method)-based acoustic holography to radiation analysis of sound sources with arbitrarily shaped geometries.
8. E. G. WILLIAMS 1999 *Fourier Acoustics, Sound Radiation and Nearfield Acoustical Holography*. New York: Academic Press.
9. Z. WANG and S. F. WU 1997 *Journal of the Acoustical Society of America* **102**, 2020–2032. Helmholtz equation-least squares method for reconstructing the Acoustic Pressure Field.
10. S. F. WU and J. YU 1998 *Journal of the Acoustical Society of America* **104**, 2054–2060. Reconstructing interior acoustic pressure fields via Helmholtz equation least-squares (HELS) method.
11. S. F. WU 2000 *Journal of the Acoustical Society of America* **107**, 2511–2522. On reconstruction of acoustic pressure fields by using HELS Method.
12. N. E. RAYESS and S. F. WU 2000 *Journal of the Acoustical Society of America* **107**, 2955–2964. Experimental validations of the HELS method for reconstructing acoustic radiation from a complex vibrating structure.
13. P. M. MORSE and H. FESHBACH 1953 *Methods of Theoretical Physics*. New York: McGraw-Hill Book Company.
14. S. F. WU, N. E. RAYES and X. ZHAO 2001 *Journal of the Acoustical Society of America* **109**, 2771–2779. Visualization of acoustic radiation from a vibrating bowling ball.